

ORIGINAL

Open Access

A facile one-step synthesis of PTSA-doped tetraaniline nanostructure/magnetite nanoparticles via self-assembly method

Keloth Basavaiah*, Yarramsetti Pavankumar and Alamanda Vara Prasada Rao

Abstract

Tetraaniline nanostructures/magnetite nanoparticles (Fe_3O_4 NPs) have been prepared via *in situ* self-assembly method using ammonium persulphate as an oxidant in the presence of *p*-toluene sulphonic acid as a dopant as well a soft template. The effect of the concentration and molar ratio of *p*-toluene sulphonic acid to aniline on the morphology and size of the nanostructures, and the crystallinity, thermal stability and magnetic properties of the nanocomposites have been studied by UV-visible spectroscopy, Fourier transform infrared spectroscopy, X-ray diffraction, scanning electron microscopy, transmission electron microscopy, thermogravimetric analysis and vibrating sample magnetometry. The spectroscopic results indicated the interaction between the tetraaniline nanostructures and the Fe_3O_4 NPs. The microscopic results show that the Fe_3O_4 NPs were coated on tetraaniline nanostructures. The saturation magnetization values and the thermal stability of the nanocomposites were found to depend on the molar ratio of *p*-toluene sulphonic acid to aniline.

Keywords: Intrinsic conducting polymer; Tetraaniline; Magnetite nanoparticles; *In situ* self-assembly; Superparamagnetism

Background

Since their discovery, intrinsic conducting polymers (ICPs) have emerged as potential materials for many technological applications due to their unique electronic properties covering the whole insulator-semiconductor-metal range, mechanical flexibility and relative ease of processing. Among the most commonly studied ICPs is polyaniline (PANI) due to its ease of synthesis, unique non-redox doping/dedoping chemistry, relatively high conductivity and environmental stability [1], and many technological applications in molecular electronics, light emitting diodes, sensors, actuators, solar cells, light weight batteries and antistatic and anticorrosion coatings [2].

Recently, PANI nanostructures such as nanotubes, nanorods, nanofibers and nanowires have attracted attention over its bulk counterpart because of their low dimensionality and high surface-to-volume ratio. PANI nanostructures have been prepared by various methods such as interfacial polymerization, plasma polymerization,

enzymatic polymerization, electrospinning and rapid mixing polymerization in the presence of specific structure-directing materials such as zeolite channels, porous membranes, opal, surfactants, polymers and bulky organic acid dopants [3-9]. In hard-template method, it is very difficult to retain ordered PANI nanostructures because harsh experimental conditions are required for the removal of hard templates [10,11]. However, the soft-template method has the advantage in preparing large quantities of PANI nanostructures by being simple and cost effective. In this method, large quantities of PANI nanostructures are produced using structure director in the form of surfactants and bulky organic acids. The external dopant acid forms complexes with monomer via the acid-base chemistry and, as a formed complex, acts as a soft template for the growth of the PANI nanostructures.

Even though PANI nanostructures have been studied extensively, a very little emphasis is given on the synthesis of the nanostructures of PANI oligomers such as

* Correspondence: kbasu@gmail.com
Department of Inorganic and Analytical Chemistry, Andhra University,
Visakhapatnam, Andhra Pradesh 530003, India

tetraaniline, octaaniline and hexadecaaniline, which have been studied experimentally and theoretically as model compounds for PANI. Among the PANI oligomers, tetraaniline (TANI) has received great attention because it is soluble in common solvents, exhibits similar electroactivity as PANI and has well-defined structure, designed end group and monodispersed molecular weight. The most useful form of PANI is emeraldine (EBPANI), which has ca. 50% amine and ca. 50% imine nitrogen, in which one of its four rings is quinoid, the remaining three being benzenoid. TANI is a perfect model compound for PANI since its chemical structure resembles that of EBPANI.

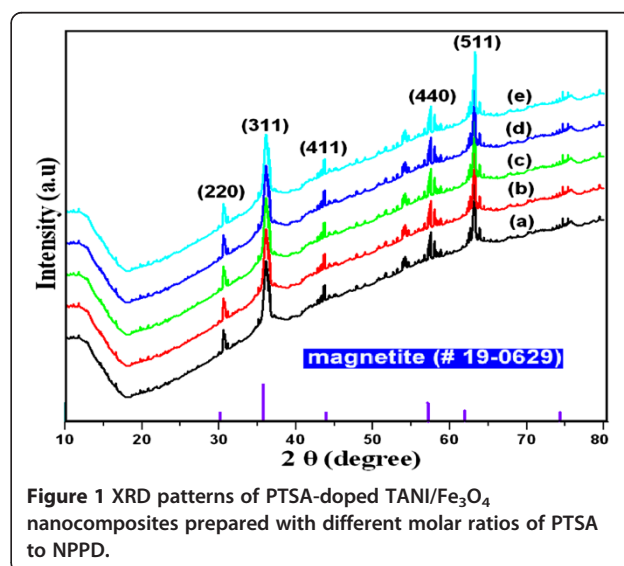
ICP nanocomposites, in particular, with magnetic nanoparticles (MNPs), have also received a great deal of attention because they are multifunctional materials with many technological applications like magnetic electrocatalysis, non-linear optic processes, electromagnetic interference shielding, antibiofouling, separation and purification of biomolecules, as carriers for targeted drug delivery and biosensors [12-15]. Among all MNPs, magnetite nanoparticles (Fe_3O_4 NPs) have attracted attention because they have many potential applications due to their low toxicity, high saturation magnetization biocompatibility. In most of these applications, magnetic nanoparticles are found to be easily dispersed in aqueous solution, which have particle sizes less than the critical size, without forming any aggregation. However, Fe_3O_4 NPs easily aggregate because of dipole-dipole interaction and van der Waals attractive forces between the nanoparticles, which results in poor magnetic properties and low dispersibility. One of the important approaches is, therefore, to overcome these limitations by protecting the Fe_3O_4 NPs with macrocyclic surfactants, polymers, inorganic metals, or oxides. The advantage of using a protective layer around each nanoparticle is that it not only avoids aggregation but also provides a platform for further functionalization. Among all the protective layer materials, PANI has received more attention. However, like other ICPs, the solution processing of PANI is difficult because of the presence of intrachain and interchain H-bonding interactions arising from the N-quinonoid and benzenoid units.

Here, we report a novel, scalable and simple one-pot synthesis of *p*-toluene sulphonic acid (PTSA)-doped TANI/ Fe_3O_4 NP nanocomposites via micelle-assisted *in situ* chemical oxidative polymerization using ammonium peroxydisulphate (APS) as an oxidant. In this technique, PTSA acts as the dopant as well as the soft template for the synthesis of TANI/ Fe_3O_4 nanocomposites. The effect of PTSA concentration and molar ratio of PTSA to monomer on the morphology, crystallinity, magnetic properties and thermal properties of the nanocomposites have been investigated.

Results and discussion

PTSA-doped TANI/ Fe_3O_4 nanocomposites have been prepared by oxidative chemical polymerization using APS as an oxidant. PTSA has been found to play a dual role in the formation of TANI nanostructures as a dopant and as a surfactant. Due to the presence of methyl group and hydrophilic '- SO_3H ' group, PTSA can form micelles in water. PTSA can also form micelles by forming a complex with NPPD via the acid-base interaction between the - SO_3H group of the PTSA and the "- NH_2 " group of the NPPD. Thus, the reaction medium consists of PTSA micelles, PTSA-NPPD micelles and free NPPD. Moreover, the concentration of the PTSA micelles, PTSA-NPPD micelles and anilinium cations present in the reaction solution is dependent on the molar ratio of PTSA to NPPD which results in the variation of morphology and size of the TANI/ Fe_3O_4 nanocomposites. As formed, the PTSA micelles or the PTSA-NPPD micelles serve as "soft template" for the growth of the TANI nanostructures. The presence of excess free PTSA can effectively prevent the formation of larger particles due to steric hindrance of bulky polymeric acids surrounding each nanoparticle and, thereby, producing nanometre-size polymer. Moreover, the hydrophilic "- SO_3 " group of PTSA limits the size of the Fe_3O_4 NPs by forming a coating layer around the particle, while the hydrophobic methyl group acts as a barrier to prevent the Fe_3O_4 NPs from aggregating, which results from the repulsive forces among the surroundings nanoparticle.

The molecular structure of the PTSA-doped TANI/ Fe_3O_4 nanocomposite was investigated by UV-visible spectroscopy, FTIR spectroscopy and powder X-ray diffraction (XRD). Figure 1a,b,c,d,e represents the powder XRD patterns of the PTSA-doped TANI/ Fe_3O_4 nanocomposites prepared with 1:1, 2:1, 3:1, 4:1 and 5:1 molar ratio of PTSA



to NPPD. The XRD patterns show both the broad amorphous peaks and sharp crystalline peaks of TANI. The broad peaks were observed at $2\theta = 19.8^\circ$ and 25° , while the sharp crystalline peaks, at $2\theta = 11^\circ$, 13° and 22° . The sharp crystalline peaks originated from the increase in the interplanar distance due to the inclusion of PTSA in the tunnels between the TANI chains. The XRD patterns centred at $2\theta = 31^\circ$, 36° , 44° , 58° and 63° can be indexed as (220), (311), (400), (511) and (440) planes of the magnetite, respectively, which are in good agreement with the standard magnetite JCPDS card (card no. 19-0629).

The UV-vis spectra of the PTSA-doped TANI/Fe₃O₄ nanocomposites prepared with 1:1, 2:1, 3:1, 4:1 and 5:1 molar ratios of PTSA to NPPD are presented in Figure 2. The UV-vis spectra of the nanocomposites dispersed in dimethyl sulphonic oxide (DMSO) show three prominent absorption bands at 285, 335 and 595 nm. The absorption band at 285 is ascribed to the $\pi \rightarrow \pi^*$ transition in the benzenoid rings of PTSA, indicating the doping of PTSA to TANI in the nanocomposites. The bands at 335 and 595 nm are due to the $\pi \rightarrow \pi^*$ transition of the benzenoid rings in the TANI chain and the transition caused by the interchain charge transfer from the two adjacent benzenoid rings to the quinoid ring of the TANI chain, respectively [16]. Both these absorption bands were shifted to the lower wavelength region from those of pure TANI, indicating that there is some interaction between Fe₃O₄ NP and TANI.

Figure 3 depicts the FTIR spectra of the PTSA-doped TANI/Fe₃O₄ nanocomposite synthesized using the different molar ratios of PTSA to NPPD (1:1, 2:1, 3:1, 4:1 and 5:1). The bands at 3,180, 1,596 and 1,493 cm⁻¹ are ascribed to the N-H stretching vibration, C=C stretching mode of quinoid phenyl and benzenoid phenyl rings, respectively. The band at 1,408 cm⁻¹ is due to the stretching frequency of the B-N=Q moiety (where B refers to

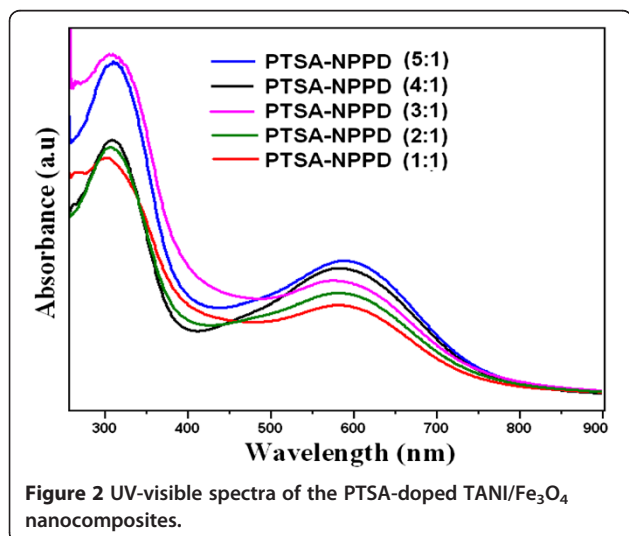


Figure 2 UV-visible spectra of the PTSA-doped TANI/Fe₃O₄ nanocomposites.

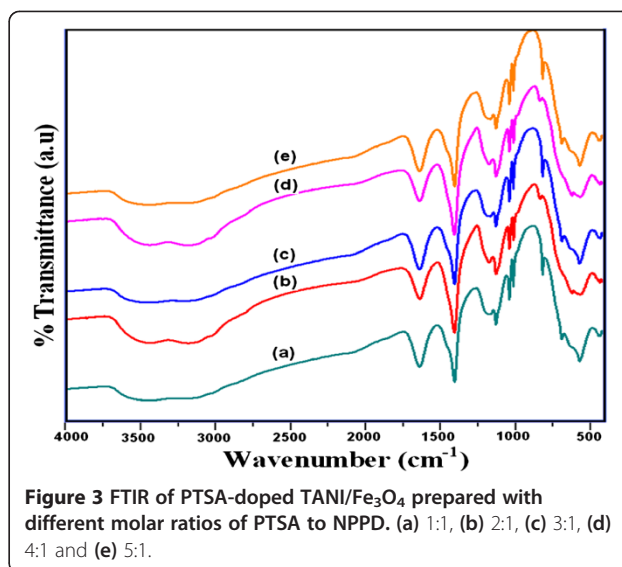


Figure 3 FTIR of PTSA-doped TANI/Fe₃O₄ prepared with different molar ratios of PTSA to NPPD. (a) 1:1, (b) 2:1, (c) 3:1, (d) 4:1 and (e) 5:1.

benzenoid phenyl rings, and Q refers to quinoid phenyl ring). The C-N stretching and the C-H aromatic in-plane and out-of-plane deformations of the 1,4-disubstituted benzene rings were confirmed by the presence of band 1,304, 1,136 and 836 cm⁻¹ [17]. The PTSA doping to TANI/Fe₃O₄ is confirmed by the presence of characteristic bands due to the symmetric and asymmetric O=S=O stretching vibrations of the -SO₃H group of PTSA (1,038 and 1,008 cm⁻¹). The bands at 580 and 454 cm⁻¹ were ascribed to the intrinsic Fe-O stretching vibrations of tetrahedral and octahedral Fe³⁺ of the magnetite nanoparticle in the nanocomposites [18].

The morphology of the TANI/Fe₃O₄ NP nanocomposites was investigated by transmission electron microscopy (TEM) and SEM. The SEM images (Figure 4) show the rod-like morphology of the PTSA-doped TANI/Fe₃O₄ nanocomposite prepared at 5:1 molar ratio of PTSA to NPPD. It can be seen from the SEM image (Figure 5) that no rod-like morphology was obtained for the PTSA-doped TANI/Fe₃O₄ nanocomposite prepared with 4:1, 3:1, 2:1 and 1:1 molar ratios of PTSA to NPPD. The presence of carbon, nitrogen, oxygen, sulphur and iron in the TANI/Fe₃O₄ nanocomposites is confirmed by energy dispersive X-ray analysis (EDAX) (Figure 5f).

Figure 6 shows the TEM images of the as-prepared PTSA-doped TANI/Fe₃O₄ nanocomposites in direct reaction dispersion and dispersion obtained from final dried powder dispersed in DMSO. The TEM image (Figure 6a) clearly reveals the rod-like morphology of the TANI/Fe₃O₄ nanocomposites prepared with the 5:1 molar ratio of PTSA/NPPD. A closer look at the nanorods reveals that the average diameter is 40 to 95 nm, and the length of the nanorods is several hundred nanometres. Figure 6b represents the TEM image of the PTSA-doped TANI/Fe₃O₄ nanocomposite after being dispersed in DMSO, which

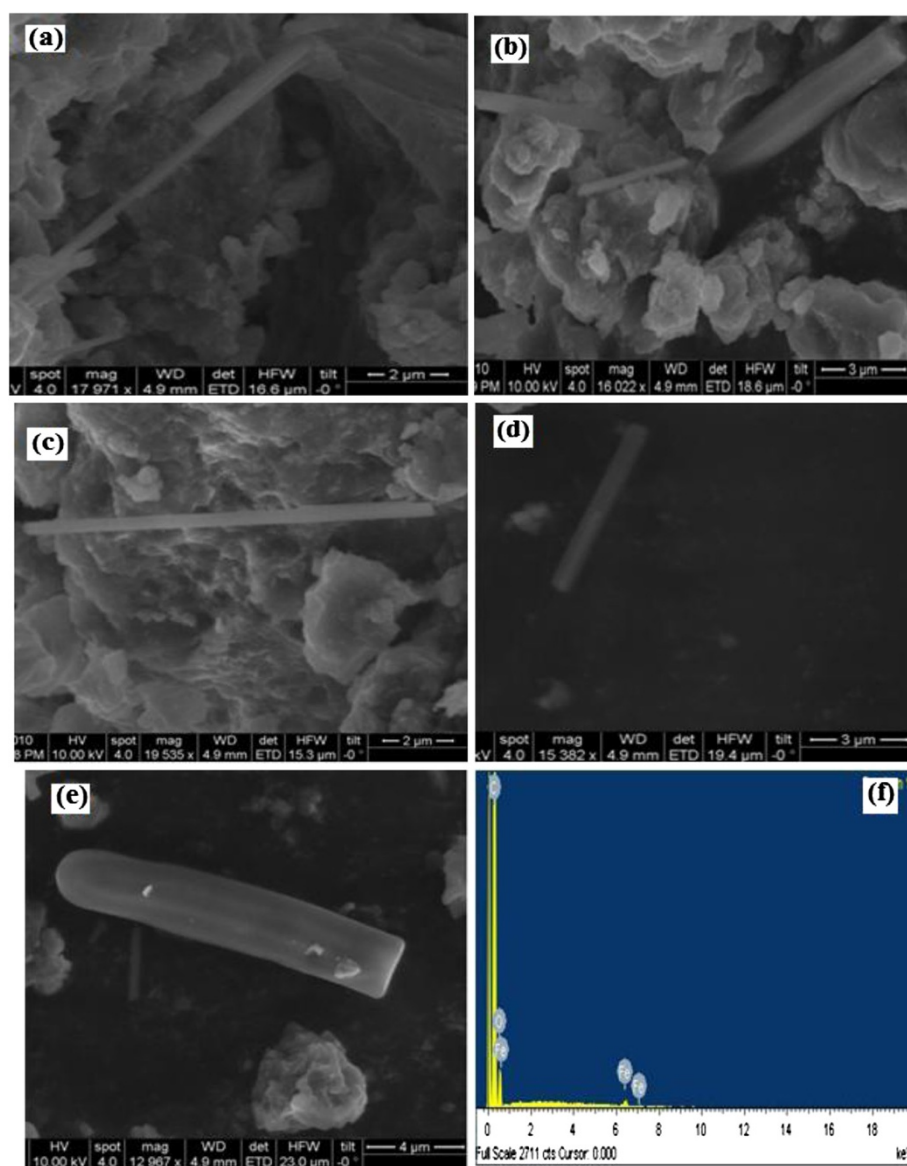


Figure 4 Images of the PTSA-doped TANI/Fe₃O₄ with the 5:1 molar ratio of PTSA/NPPD. (a, b, c, d and e) SEM and (f) EDX.

shows spherical Fe₃O₄ NPs in the composite with average size of 7 to 10 nm. The TEM images of the PTSA-doped TPANI/Fe₃O₄ nanocomposite samples prepared with 4:1, 3:1, 2:1 and 1:1 molar ratios of PTSA to NPPD are presented in Additional file 1: Figure S1, which show spherical nanoparticles without any aggregation. The SAED patterns (see in Additional file 1: Figure S2) show sharp, well-defined diffraction rings, which reveal the crystallinity of the Fe₃O₄ NPs. The corresponding interplanar spacing calculated from the diffraction patterns matched with that of the standard bulk Fe₃O₄ (JCPDS, card no. 19-0629).

The room temperature field-dependent magnetization curves of the PTSA-doped TANI/Fe₃O₄ nanocomposites

prepared with 5:1,4:1, 3:1, 2:1 and 1:1 molar ratios of PTSA to NPPD are shown in Figure 7. The nanocomposite samples exhibited superparamagnetic behaviour as evidenced by zero remanence, zero coercivity and the absence of hysteresis loops. The saturation magnetization (*M_s*) values of the PTSA-doped TANI/Fe₃O₄ are 46, 34, 33, 32 and 10 emu g⁻¹, corresponding to 1:1, 2:1, 3:1, 4:1 and 5:1 PTSA-to-NPPD molar ratios. The *M_s* values are much lower than the theoretical *M_s* values of bulk magnetite of 92 emu g⁻¹ [19]. The decrease of the *M_s* values is due to the finite size effect and surface effect. Below the critical particle size, the total magnetization decreases due to increased dispersion in the exchange integral and finally approaches the

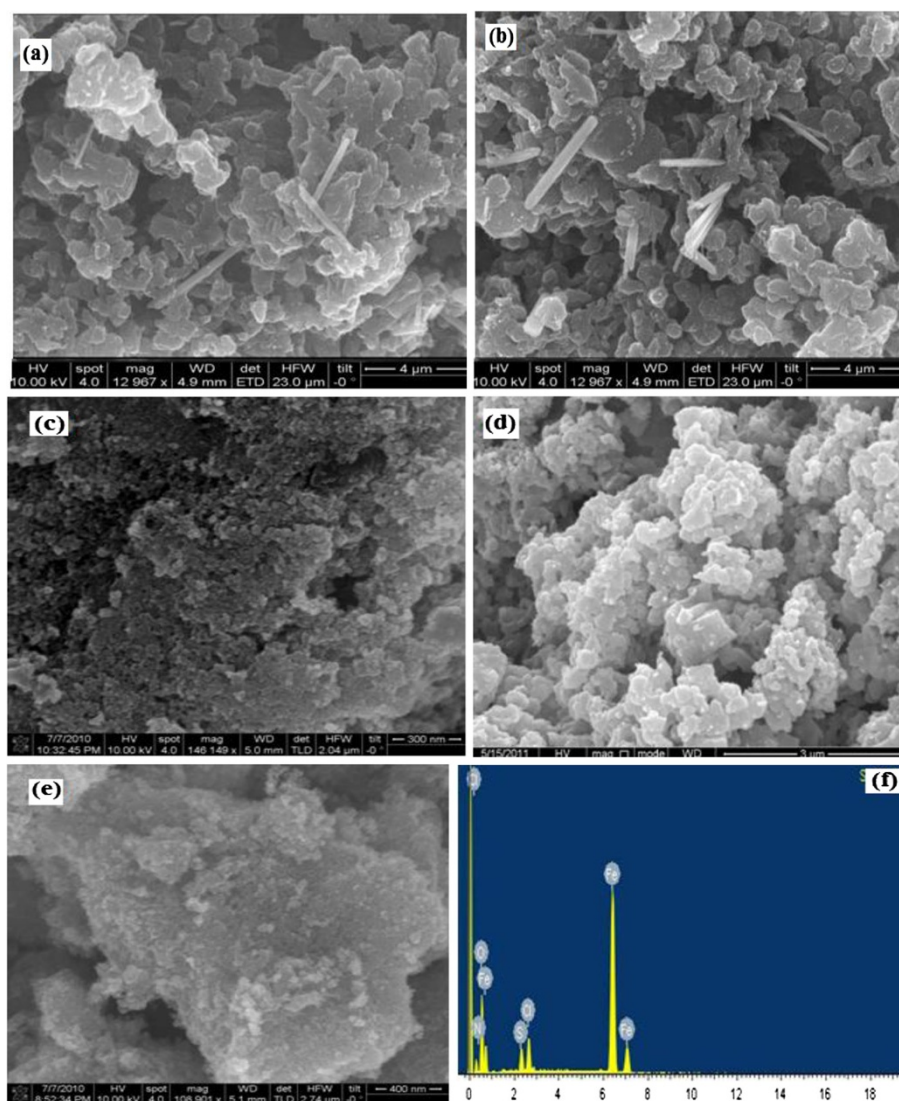


Figure 5 Images of the PTSA-doped TANI/ Fe_3O_4 nanocomposites prepared with different molar ratios of PTSA to NPPD. The nanocomposites in (a) and (b) 4:1, (c) 3:1, (d) 2:1, (e) 1:1 molar ratios. (f) EDX of the PTSA-doped TPANI/ Fe_3O_4 .

superparamagnetic state. The decrease of the M_s values may also be due to the increase of the weight ratio of the non-magnetic PTSA and TANI in the nanocomposites.

Figure 8 shows the TGA curve of the pure TANI and PTSA-doped TANI/ Fe_3O_4 nanocomposites prepared with various molar feed ratios of PTSA to NPPD under N_2 atmosphere at a heating rate $20^\circ\text{C}/\text{minute}$ in the temperature range of 50°C to 840°C . A close comparison of the thermal transitions between them revealed that the TANI/ Fe_3O_4 nanocomposites are more thermally stable than pure TANI. Three characteristic weight loss regions were observed for both pure TANI and all PTSA-doped TANI/ Fe_3O_4 nanocomposites. The first weight loss before 130°C corresponds to the removal of water, excess of unbound PTSA and other

volatile impurities in the composites. The second stage of weight loss below 350°C is associated to the loss of bound PTSA and the decomposition of TANI initiated by the dopant acid. The final continuous weight loss occurring between 350°C and 650°C is attributed to the breakdown of the main chain of TANI. The TGA curves of the composites revealed higher final residue and better thermal stability due to the higher packing of TANI and the retarding effect of Fe_3O_4 NPs, respectively.

Conclusions

PTSA-doped TANI/ Fe_3O_4 nanocomposites were prepared by *in situ* oxidative chemical polymerization technique using APS, an oxidant, via micelle-assisted self-assembly method. The SEM and TEM images clearly show that the

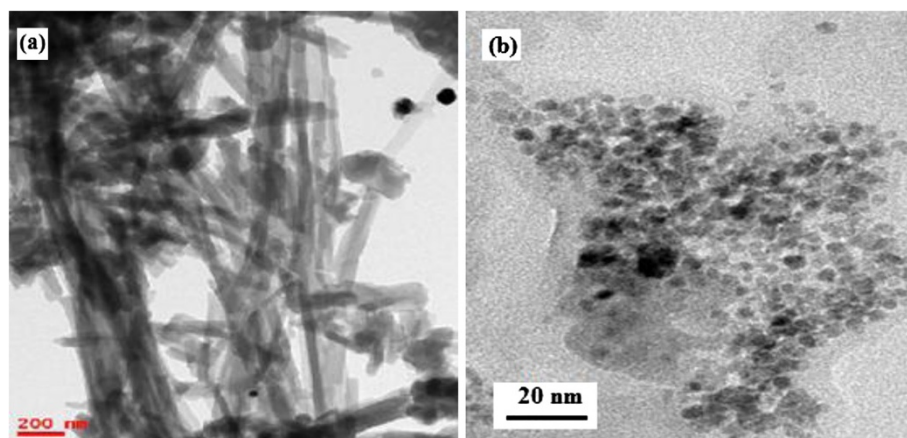


Figure 6 TEM images of the PTSA-doped TANI/Fe₃O₄ nanocomposites. (a) Crude and (b) dispersed nanocomposites.

Fe₃O₄ NPs were coated on the surface of the TANI nanostructures. The morphology, crystallinity, magnetic properties and thermal stability of the nanocomposites were found to be dependent on the concentration and molar ratio of PTSA to NPPD. Magnetic studies show superparamagnetic behaviour, with saturation magnetization values much lower than those for bulk magnetite. The TANI/Fe₃O₄ nanocomposites showed higher thermal stability as compared to pure TANI, indicating the interaction between Fe₃O₄ NPs and TANI in the nanocomposites.

Methods

Materials

N-phenyl-1,4-phenyldiamine (NPPD) and PTSA were obtained from Aldrich Chemical Company (Milwaukee, USA) and were used as received without further purification. APS ((NH₄)₂S₂O₈), FeCl₃·6H₂O, FeSO₄·7H₂O, ammonia (NH₃-H₂O), sodium hydroxide and methanol

were purchased from Merck & Co., Inc. (Bengaluru, India) and were used as received without any purification. All other reagents were of analytical grade and used without further purification. Milli-Q (EMD Millipore Corporation, Billerica, MA, USA) water with resistance greater than 18 MΩ was used for the preparation of all solutions.

Synthesis of TANI nanorods/ Fe₃O₄ NPs composites

PTSA-doped TANI/Fe₃O₄ nanocomposites were prepared via *in situ* oxidative chemical polymerization method using APS as an oxidant. In a typical synthesis process, 0.1840 g of NPPD was dissolved in 50 mL of Milli-Q water and then 1.9105 g of PTSA was added in under vigorous stirring. The reaction mixture was quickly cooled at 0°C to 5°C using ice-water bath with constant stirring for 2 h. Then, a pre-cooled solution of 1 mL aqueous APS (1 mol L⁻¹) was added dropwise to the above under vigorous stirring. The colour of the

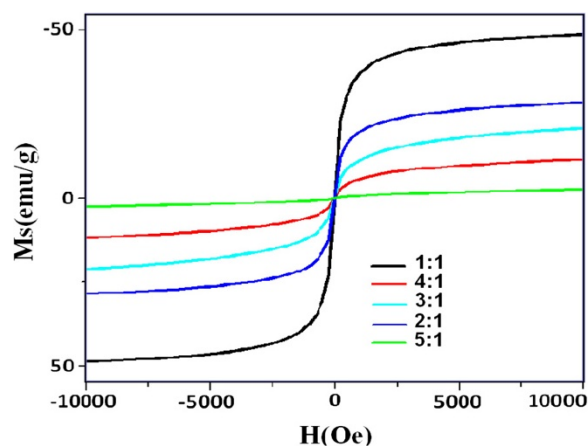


Figure 7 Variation of magnetization as a function of field for PTSA-doped TANI/Fe₃O₄ nanocomposite samples.

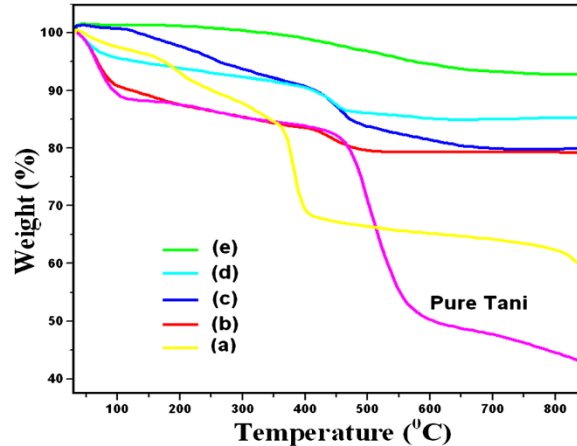


Figure 8 TGA curve of the pure TANI and PTSA-doped TANI/Fe₃O₄ nanocomposites.

reaction mixture slowly turns from colourless to light blue and finally to dark green. The reaction is allowed to proceed for 5 h at 0°C to 5°C before allowing it to attain room temperature. To the above reaction mixture, 10 mL of 1 mol L⁻¹ FeCl₃·6H₂O and 10 mL of 0.5 mol L⁻¹ FeSO₄·7H₂O aqueous solutions were added at 75°C under stirring and then 5 mL of 25% NH₄OH solution was added. The colour of the reaction mixture turns black, indicating the formation of magnetite. The reaction was allowed to proceed for 5 h under vigorous stirring until TANI/Fe₃O₄ dispersion was obtained. The as-synthesized nanocomposites were centrifugated and washed with a large amount of distilled water and then with methanol. Finally, the product was dried under vacuum at 50°C for 5 h. The same procedure has been adopted for the preparation of all PTSA-doped TANI/Fe₃O₄ composites while varying the molar ratio of PTSA to NPPD from 5:1 to 1:1.

Characterization

Powder XRD patterns were recorded using a Siemens AXS D5005 X-ray diffractometer (Mumbai, India) using CuK α radiation (λ = 1.54 Å) at 5°/min. Fourier transform infrared (FTIR) spectra were recorded on a PerkinElmer SPECTRUM 1000 FTIR Spectrometer (Thane, India) over the range of 400 to 4,000 cm⁻¹. The powder samples were mixed thoroughly with KBr and pressed into transparent pellets. The morphology is investigated with a JEOL JSM6610 LV scanning electron microscope (SEM, Tokyo, Japan) equipped with an electron probe microanalyzer and a FEI TECNAI G2 S-Twin transmission electron microscope (Hillsboro, OR, USA) at accelerating voltages of 120 and 200 kV. The samples for SEM were mounted on aluminium studs and gold coated prior to imaging. EDAX was also performed with the same equipment to determine elemental analysis. For the TEM measurements, the powders were ultrasonicated in DMSO, and a drop of the suspension was dried on a carbon-coated microgrid. For UV-visible absorption spectra, the samples were dissolved in DMSO, and the spectra were recorded on a PerkinElmer double beam LS-50 spectrophotometer. The room temperature magnetization in the applied magnetic field was performed using vibrating sample magnetometer. Thermogravimetric analysis (TGA) was conducted with a Cahn TG131 TGA system (Cerritos, CA, USA) at a heating rate of 20°C/min under nitrogen atmosphere from room temperature to 850°C.

Additional file

Additional file 1 Figure S1 and S2. TEM images and SAED patterns of the PTSA-doped TANI/Fe₃O₄ nanocomposites.

Competing interests

The authors declare that they have no competing interests.

Authors' contributions

KB and YP carried out the synthesis and characterization of the nanocomposites. KB and AVPR prepared the manuscript. YP carried out the magnetic and thermal studies. All authors read and approved the final manuscript.

Authors' information

AVPR is a professor at the Department of Inorganic & Analytical Chemistry, Andhra University, India. He received his PhD degree in Solid State Chemistry from Pennsylvania State University, USA. His current research has focused on solid state synthesis of various nanostructural materials. KB is an assistant professor at the Department of Inorganic & Analytical Chemistry, Andhra University, India. He obtained his MS degree from the University of Hyderabad in 2004. He received his PhD degree in organic-inorganic nanohybrid materials for catalysis and antimicrobial application. Currently, he is working on nanocomposites of one-dimensional conducting polymer and metal, metal oxide nanoparticle for various technological applications. YP received his MS degree in Analytical Chemistry from Andhra University in 2010. Currently, he is working on semiconductor nanostructure materials for environmental applications.

Acknowledgements

This work was supported by the University Grant Commission, India (UGC, India) under major research project. YPK thanks UGC, India for the award of research fellowship. The authors are grateful to Prof. TP Radhakrishnan and Muvva D. Prasad, Centre for Nanotechnology, University of Hyderabad, for providing the TEM facility.

Received: 29 May 2013 Accepted: 11 July 2013

Published: 29 Aug 2013

References

1. Lee, K, Cho, S, Park, SH, Heeger, AJ, Lee, CW, Lee, SH: Metallic transport in polyaniline. *Nature* **441**, 65–68 (2006)
2. Sfez, R, De-Zhong, L, Turyan, I, Mandler, D, Yitzchaik, S: Polyaniline Monolayer Self-Assembled on Hydroxyl-Terminated Surfaces. *Langmuir* **17**, 2556 (2001)
3. Choi, J, Kim, SJ, Lee, J, Lim, JH, Lee, SC, Kim, KJ: Controlled self-assembly of Nanoporous alumina for the self-templating synthesis of polyaniline nanowires. *Electrochem Commun* **9**, 971–975 (2007)
4. Li, GR, Feng, ZP, Zhong, JH, Wang, ZL, Tong, YX: Electrochemical Synthesis of Polyaniline Nanobelts with Predominant Electrochemical Performances. *Macromolecules* **43**, 2178–2183 (2010)
5. Chen, J, Chao, D, Lu, X, Zhang, W: Novel interfacial polymerization for radially Oriented polyaniline nanofibers. *Mater Lett* **61**, 1419–1423 (2007)
6. Nastase, F, Stamatini, I, Nastase, C, Mihaiescu, D, Moldovan, A: Synthesis and characterization of PANi-SiO₂ and PTH-SiO₂ nanocomposites thin films by plasma polymerization. *Prog Solid State Chem* **34**, 191199 (2006)
7. Cruz-Silva, R, Ruiz-Flores, C, Arizmendi, L, Romero-Garci, J, Arias-Marin, E, Moggio, I, Castillon, FF, Farias, MH: Enzymatic synthesis of colloidal polyaniline particles. *Polymer* **47**, 1563–1568 (2006)
8. Hou, H, Jin, Z, Reuning, A, Schaper, A, Wendorff, JH, Greiner, A: Poly(p-xylylene) Nanotubes by Coating and Removal of Ultrathin Polymer Template Fibers. *Macromolecules* **119**, 27 (2002)
9. Huang, JX, Kaner, RB: Nanofiber Formation in the Chemical Polymerization of Aniline: A Mechanistic Study. *Angew Chem Int Ed* **43**, 5817–5821 (2004)
10. Zhang, X, Manohar, SK: Polyaniline nanofibers: chemical synthesis using surfactants. *Chem Commun* **20**, 2360–2361 (2004)
11. Chiou, NR, Lee, LJ, Epstein, AJ: Porous membrane controlled polymerization of nanofibers of polyaniline and its derivatives. *J Mater Chem* **18**, 2085–2089 (2008)
12. Gangopadhyay, R, De, A: Conducting Polymer Nanocomposites: A Brief Overview. *Mater* **12**, 608–622 (2000)
13. Meldrum, FC, Heywood, BR, Mann, S: Magnetoferritin: in vitro synthesis of a novel magnetic protein. *Science* **257**, 522–523 (1992)
14. Martin, CR, Mitchell, DT: Nanomaterials in Analytical Chemistry. *Anal Chem* **70**, 322A–327A (1998)
15. Murthy, N, Thng, YX, Schuck, S, Xu, MC, Frechet, JMJ: A Novel Strategy for Encapsulation And Release of Proteins: Hydrogels and Microgels with Acid-Labile Acetal Cross-Linkers. *J Am Chem Soc* **124**, 12398–12399 (2002)
16. Li, XG, Li, A, Huang, MR: Facile High-Yield Synthesis of Polyaniline Nanosticks with Intrinsic Stability and Electrical Conductivity. *Chem Eur J* **14**, 10309–10317 (2008)

17. Abdiryim, T, Xiao-Gang, Z, Jamal, R: Comparative studies of solid-state synthesized Polyaniline doped with inorganic acids. *Mater Chem Phys* **90**, 367–372 (2005)
18. Waldron, RD: Infrared spectra of ferrites. *Phys Rev* **99**, 1727–1735 (1955)
19. Popple Well, J, Sakhnini, L: The dependence of physical and magnetic properties of Magnetic fluids on particle size. *J Magn Magn Mater* **142**, 72–78 (1995)

10.1186/2193-8865-3-74

Cite this article as: Basavaiah *et al.*: A facile one-step synthesis of PTSA-doped tetraaniline nanostructure/magnetite nanoparticles via self-assembly method. *Journal Of Nanostructure in Chemistry* 2013, **3**:74

Submit your manuscript to a SpringerOpen[®] journal and benefit from:

- Convenient online submission
- Rigorous peer review
- Immediate publication on acceptance
- Open access: articles freely available online
- High visibility within the field
- Retaining the copyright to your article

Submit your next manuscript at ► springeropen.com